New Charge Transfer Salts Based on Bis(ethylenedithio)tetrathiafulvalene (ET) and Ferro- or Antiferromagnetic Oxalato-Bridged Dinuclear Anions: Syntheses, Structures and Magnetism of $ET_5[MM'(C_2O_4)(NCS)_8]$ with $MM' = Cr^{III}Fe^{III}$, $Cr^{III}Cr^{III}$

Smaïl Triki,*,† Florence Bérézovsky,† Jean Sala Pala,† Carlos J. Gómez-García,‡ Eugenio Coronado,‡ Karine Costuas,§ and Jean-François Halet§

UMR CNRS 6521, Chimie, Electrochimie Moléculaires, Chimie Analytique, Université de Bretagne Occidentale, BP 809, 29285 Brest Cedex, France, Instituto de Ciencia Molecular, Universidad de Valencia, Dr Moliner 50, 46100 Burjasot, Spain, and Laboratoire de Chimie du Solide et Inorganique Moléculaire, UMR CNRS 6511, Université de Rennes 1, Institut de Chimie de Rennes, 35042 Rennes Cedex, France

Received February 16, 2001

Electrochemical combination of the magnetic dinuclear anion $[MM'(C_2O_4)(NCS)_8]^{4-}$ ($MM' = Cr^{III}Cr^{III}$, Cr^{III}-Fe^{III}) with the ET organic π-donor (ET = BEDT−TTF = bis(ethylenedithio)tetrathiafulvalene) gives rise to two new isostructural molecular hybrid salts $ET_5[MM'(C_2O_4)(NCS)_8]$, with $MM' =$ CrCr (**1**), CrFe (**2**). The molecular structure of compound **1** has been determined by single crystal X-ray diffraction. The particular arrangement of the organic units consists of an unprecedented two-dimensional organic sublattice nearly similar to that observed in κ-phase structures. For both compounds, the magnetic susceptibility measurements indicate (i) the ET radicals do not contribute to the magnetic moment probably due to the presence of strong antiferromagnetic interaction between them, and (ii) in the anion, the magnetic coupling is antiferromagnetic for **1** ($J = -3.65$ cm^{-1}) and ferromagnetic for **2** ($J = 1.14$ cm^{-1}, J being the parameter of the exchange Hamiltonian $H = -2JS_1S_2$). The field dependence of the magnetization of compound **2** at 2.0 K gives further evidence of the $S = 4$ ground-state arising from the interaction between $S = 3/2$ Cr(III) and $S = 5/2$ Fe(III). EPR measurements confirm the nature of the magnetic interactions and the absence of any contribution from the organic part, as observed from the static magnetic measurement. Conductivity measurements and electronic band structure calculations show that both salts are semiconductors with low activation energies.

Introduction

Radical cation salts derived from the π organic donor ET (ET = BEDT−TTF = bis(ethylenedithio)tetrathiafulvalene) have attracted considerable interest because of the rich variety of their organic packing and the two-dimensionality of their electronic structures (essentially for β and κ phases), affording various solid-state properties, such as superconductivity.[1] Almost all these systems incorporate simple diamagnetic anions. In contrast, molecular organic/inorganic hybrid materials in which these anions are metal complexes with the ability to introduce a second property in the material, such as magnetism[2−12] or photochromism,[13] only very recently have begun to be explored. To obtain such materials, organic π donors are combined with a variety of complex molecular anions such as tris(oxalato)metalates,[2,3] tetrahalogenometalates,[4−7] hexacyanometalates,[8] hexathiocyanatometalates,[9] and polyoxometalates.[10−12] The most significant achievements obtained in this field are sequentially the discovery of coexistence of paramagnetism/metallic conductivity,[4] paramagnetism/superconductivity,[2] antiferromagnetism/superconductivity,[14] ferromagnetism/metallic conductivity,[15] and very recently, field-induced ferromagnetism/superconductivity.[16]

* To whom correspondence should be addressed. E-mail: triki@univ-brest.fr.

† University of Brest.

‡ University of Valencia.

§ University of Rennes 1.

(1) Williams, J. M.; Ferraro, J. R.; Thorn, R. J.; Carlson, J. D.; Geiser, U.; Wang, H. H.; Kini, A. M.; Whangbo, M. H. In *Organic Superconductor. Synthesis, Structure, Properties and Theory*; Grimes, R. N., Ed.; Prentice Hall: Englewood Cliffs, New Jersey, 1992.

(2) Kurmoo, M.; Graham, A. W.; Day, P.; Coles, S. J.; Hursthouse, M. B.; Caulfield, J. L.; Singleton, J.; Pratt, F. L.; Hayes, W.; Ducasse, L.; Guionneau, P. *J. Am. Chem. Soc.* **1995**, *117*, 12209.

(3) Martin, L.; Turner, S. S.; Day, P.; Mabbs F. E.; McInnes, E. J. L. *J. Chem. Soc., Chem. Commun.* **1997**, 1367.

(4) Day, P.; Kurmoo, M.; Mallah, T.; Marsden, I. R.; Friend, R. H.; Pratt, F. L.; Hayes, W.; Chasseau, D.; Gaultier, J.; Bravic, G.; Ducasse, L. *J. Am. Chem. Soc.* **1992**, *114*, 10722.

(5) Kobayashi, H.; Tomita, H.; Naito, T.; Kobayashi, A.; Sakai, F.; Watanabe, T.; Cassoux, P. *J. Am. Chem. Soc.* **1996**, *118*, 368.

(6) Tanaka, H.; Adachi, T.; Ojima, E.; Fujiwara, H.; Kato, K.; Kobayashi, H. *J. Am. Chem. Soc.* **1999**, *121*, 11243.

(7) Coronado, E.; Falvello, L. R.; Galán-Mascarós, J. R.; Giménez-Saiz, C.; Gómez-García, C. J.; Lauhkin, V. N.; Pérez-Benítez, A.; Rovira, C.; Veciana, J. *Adv. Mater.* **1997**, *9*, 984.

(8) Le Maguerès, P.; Ouahab, L.; Briard, P.; Even, J.; Bertault, M.; Toupet, L.; Ramos, J.; Gómez-García, C. J.; Delhaès, P.; Mallah, T. *Synth. Met.* **1997**, *86*, 1859.

(9) Bérézovsky, F.; Triki, S.; Sala Pala, J.; Galán-Mascarós, J. R.; Gómez-García, C. J.; Coronado, E. *Synth. Met.* **1999**, *102*, 1755.

(10) Gómez-García, C. J.; Giménez-Saiz, C.; Triki, S.; Coronado, E.; Le Maguerès, P.; Ouahab, L.; Ducasse, L.; Sourisseau, C.; Delhaes, P. *Inorg. Chem.* **1995**, *34*, 4139.

(11) Coronado, E.; Galán-Mascarós, J. R.; Giménez-Saiz, C.; Gómez-García, C. J.; Triki, S. *J. Am. Chem. Soc.* **1998**, *120*, 4671.

(12) Coronado, E.; Gómez-García, C. J. *Chem. Rev.* **1998**, *98*, 273.

(13) Clemente-León, M.; Coronado, E.; Galán-Mascarós, J. R.; Canadell, E. *Inorg. Chem.* **2000**, *39*, 5394.

(14) Fujiwara, H.; Fujiwara, E.; Nakazawa, Y.; Narymbetov, B. Z.; Kato, K.; Kobayashi, H.; Kobayashi, A.; Tokumoto, M.; Cassoux, P. *J. Am. Chem. Soc.* **2001**, *123*, 306.

10.1021/ic010197b CCC: $20.00
Published on Web 08/24/2001

Notice that all these achievements are concentrated in a few examples, but their discoveries have required a significant synthetic effort in which BEDT−TTF type donors have been combined with magnetic counterions of different shapes, sizes, charges, and dimensionalities. Taking into account the crucial role of the inorganic anions in the conducting and magnetic properties of such molecular organic/inorganic hybrids, our strategy lies in combining metal complexes containing sulfur atoms with ET donors with the aim of favoring the intermolecular contacts through the sulfur atoms of the ET units. In this context, we have previously developed syntheses of tetraethylammonium salts of the new oxalato bridged magnetic anions $[MM'(C_2O_4)(NCS)_8]^{4-}$ ($MM' = Cr^{III}Cr^{III}$, $Fe^{III}Fe^{III}$ and $Cr^{III}Fe^{III}$) containing isothiocyanato ligands.[17] The electrochemical combination of the homometallic and bimetallic dinuclear anions with ET led to two new isostructural radical cation salts, namely $ET_5[MM'(C_2O_4)(NCS)_8]$ ($MM' = CrCr$ (**1**); $MM' = CrFe$ (**2**)), with an unprecedented bidimensionnal ET packing. We describe here the synthesis, crystal and electronic band structures, and magnetic properties of these salts. A preliminary account of this work has already been communicated.[18] Related studies with the homodinuclear oxalato bridged anion $[Fe^{III}_2(C_2O_4)_5]^{4-}$ have been recently reported.[19,20]

Experimental Section

Syntheses of the Salts 1−2. The two radical salts (**1**−**2**) were obtained on a platinum wire electrode by anodic oxidation of the organic donor ET (2.6×10^{-3} M in a 1/1 C_6H_5CN/CH_3CN mixture) in an U-shaped electrocrystallization cell under a low current density of 0.5 $\mu A.cm^{-2}$ in the presence of the corresponding tetraethylammonium salt as supporting electrolyte (3.8×10^{-3} M in the same solvent mixture). These starting salts were synthesized according to ref 17. Two successive crystallizations of the precursor salts in acetonitrile, prior to their use in electrochemical cells, yielded well formed single crystals whose purity was checked by metal analysis and IR spectroscopy. After two weeks of electrochemical oxidation, amber platelike single crystals (**1** and **2**) were obtained from the two dinuclear anions. In each case, they were washed with acetonitrile and acetone, to remove any portion of the tetraethylammonium salt of the corresponding anion, and air-dried.

Physical Techniques. Elemental analyses were obtained from the Service Central d'Analyses, CNRS, Vernaison, France. Infrared spectra were recorded in the range 4000−200 cm^{-1} using a Perkin-Elmer 1430 spectrometer with samples prepared as KBr pellets. The magnetic studies were carried out on powder samples enclosed in medical caps. The magnetic susceptibility measurements were performed at 0.1 T after zero field cooling, in the temperature range 2−300 K with a SQUID magnetometer MPMS-XL-5 from Quantum Design. The molar susceptibility was corrected from the sample holder and diamagnetic contributions of all atoms (Pascal tables). Variable temperature ESR spectra were recorded at X-band, with a Bruker ELEXYS E500 spectrometer equipped with a helium cryostat. Temperature dependence of conductivity over the range 210−300 K was performed on single crystals using the standard four-contact d.c. method. Contacts to the crystals were made by platinum wires (25 μm diameter) attached with graphite paste. Extended Hückel tight-binding band structure calculations[21] were carried out with the program YAeHMOP[22] using standard atomic parameters for H, C, and S.

Table 1. Crystallographic Data for $ET_5[Cr_2(C_2O_4)(NCS)_8]$ (**1**)

chemical formula[a]	$C_{60}H_{40}N_8O_4S_{48}Cr_2$
formula weight[a]	2580.10
space group	*P*-1 (N° 2)
a (Å)	12.660(5)
b (Å)	12.812(7)
c (Å)	16.290(5)
α (°)	109.89(3)
β (°)	97.93(3)
γ (°)	97.47(3)
V(Å^3)	2416(4)
ρ_{calc} (g cm^{-3})	1.77
T (K)	296
[a]*Z*	1
μ (cm^{-1})	12.66
[b]$R(F_0)$	0.071
[c]$R_w(F_0)$	0.094

[a] There is 0.5 chemical formula in the asymmetric unit. [b] $R = \sum|F_o - F_c|/F_o$. [c] $R_w = [(\sum wF_o - F_c)^2/w(F_o)^2]^{1/2}$.

X-ray Crystallography. Preliminary studies showed that the two salts were isostructural, with $a = 12.660(5)$, $b = 12.812(7)$, $c = 16.290(5)$ Å, $\alpha = 109.89(3)$, $\beta = 97.93(3)$, and $\gamma = 97.47(3)°$ for **1**; $a = 12.722(8)$, $b = 12.830(8)$, $c = 16.291(9)$ Å, $\alpha = 109.81(5)$, $\beta = 97.79(5)$, and $\gamma = 97.93(5)°$ for **2**. A black platelike single crystal of **1** with dimensions $0.12 \times 0.11 \times 0.08$ mm^3 was mounted on an Enraf−Nonius CAD4 automatic diffractometer with graphite-monochromator Mo Kα radiation ($\lambda = 0.71073$ Å). Cell dimensions were obtained from 23 reflections, with a 2θ angle in the range 9.50−19.50°. A total number of 10990 reflections were collected (*h*, 0 to 16; *k*, −16 to 16; *l*, −20 to 20) in the 2θ range 5−54° using $\theta/(2-\theta)$ scan mode. During the data collection, three standard reflections were measured every 120 min and showed no significant decay. No absorption correction was applied. The structure was solved by SIR92, and successive Fourier difference syntheses led to the location of all non-hydrogen atoms. Except for the disordered carbon atom [C(30) and C(31) positions], all non-hydrogen atoms were refined on *F* by weighted anisotropic full-matrix least-squares methods using 3119 reflections with $I = 3\sigma(I)$. For the disordered carbon, both positions were finally refined independently in isotropic approximation with 50% occupancy factors. The hydrogen atoms bonded to the carbon atoms of the two ordered organic units were calculated [C−H = 0.95 Å]; the thermal parameters were taken as $U_{iso} = 1.3U_{eq}(C)$ and thereafter included as a fixed contribution to F_c. Scattering factors and corrections for anomalous dispersion were taken from ref 23; drawings were made with ORTEP,[24] and all calculations were performed on an Alphastation 255 4/233 computer using the OpenMoleN package.[25] Brief crystal data are listed in Table 1. Complete crystallographic details for the structure are included in the Supporting Information.

Results and Discussion

Crystal Structure of $ET_5[Cr_2(C_2O_4)(NCS)_8]$ (1). Since preliminary studies indicated that compounds **1** and **2** were isostructural, single crystal structure determination was only performed on compound **1**. The crystal structure determination shows that the asymmetric unit in **1** is built up of a dinuclear anion located at (1/2, 1/2, 1/2) and three crystallographically independent ET units (*A*, *B*, and *C*); the *A* and *B* units are located on general positions, whereas the *C* unit is located at the origin.

(15) Coronado, E.; Galán-Mascarós, J. R.; Gómez-García, C. J.; Laukhin, V. *Nature* **2000**, *408*, 447.
(16) Uji, S.; Shinagawa, H.; Yakabe, T.; Terai, Y.; Tokumoto, M.; Kobayashi, A.; Tanaka, H.; Kobayashi, H. *Nature* **2000**, *410*, 908.
(17) Triki, S.; Bérézovsky, F.; Sala Pala, J.; Coronado, E.; Gómez-García, C. J.; Clemente, J. M.; Riou, A.; Molinié, P. *Inorg. Chem.* **2000**, *39*, 3771.
(18) Triki, S.; Bérézovsky, F.; Sala Pala, J.; Riou, A.; Molinié, P. *Synth. Met.* **1999**, *103*, 1974.
(19) Coronado, E.; Galán-Mascarós, J. R.; Gómez-García, C. J. *J. Chem. Soc., Dalton Trans.* **2000**, 205.
(20) Rashid, S.; Turner, S. S.; Day, P.; Light, M. E.; Hursthouse, M. B. *Inorg. Chem.* **2000**, *39*, 2426.
(21) Hoffmann, R. *J. Chem. Phys.* **1963**, *39*, 1397. Whangbo, M.-H.; Hoffmann, R. *J. Am. Chem. Soc.* **1978**, *100*, 6093.
(22) Landrum, G. A. *YAeHMOP−Yet Another Extended Huckel Molecular Orbital Package*; Ithaca, New York, 1997; Version 2.0.
(23) *International Tables for X-ray Crystallography*; Kynoch, Birmingham, UK., 1974; Vol. IV.
(24) Johnson, C. K. *ORTEP*; Rep. ONL-3794: Delft, the Netherlands, 1985.
(25) Fair, C. K. *MolEN, An Interactive Intelligent System for Crystal Structure Analysis*, User Manual; Enraf-Nonius: Delft, The Netherlands, 1990.

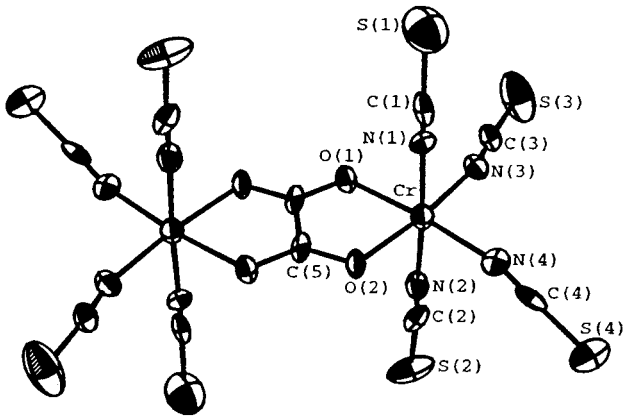

Figure 1. Structure of the dinuclear anion $[Cr_2(C_2O_4)(NCS)_8]^{4-}$ in **1** (50% probability ellipsoids). Selected distances (Å): Cr···Cr 5.253(4), Cr−O1 2.011(9), Cr−N1 2.04(1), Cr−O2 2.02(1), Cr−N2 2.01(1), C5−O1 1.25(2), Cr−N3 1.99(1), C5−O2 1.24(2), Cr−N4 1.98(1).

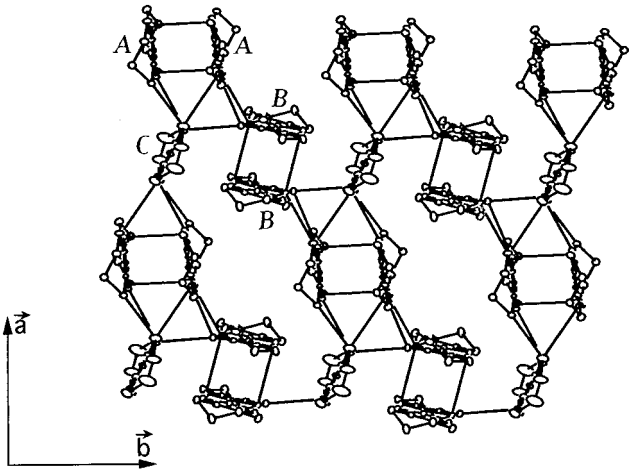

Figure 2. ORTEP view showing the crystal packing of the organic sublattice (30% probability ellipsoids) and the shortest S···S distances (<3.60 Å) between the ET units in **1**.

The complex anion is made of two chromium cations bridged by a nearly planar bis(bidentate) oxalate ligand, each metal cation is also coordinated to four isothiocyanate groups to complete its octahedral environment (Figure 1). The Cr−Cr intradinuclear distance (5.25 Å) is close to that observed for the unique example of oxalate bridged Cr(III) complexes structurally characterized (5.32 Å in $(Et_4N)_4[Cr_2(C_2O_4)_5]$-$0.2CHCl_3$).[26] The structure consists of layers of organic units parallel to the *ab* plane which are interleaved by the inorganic anions. The ET-donor network (Figure 2) contains two types of centrosymmetric dimers, *A*−*A* and *B*−*B*, and centrosymmetric ET units, *C*. Within each dimer, the overlap mode is of the so-called bond-over-ring type, similar to that observed in almost all *κ*-phases (Figure 3).[1] Careful analysis of intradimer S···S distances reveals that interactions between ET units are stronger in *A*−*A* than in *B*−*B* dimers. Adjacent *A*−*A* and *B*−*B* dimers are approximately perpendicular to each other with a dihedral angle of 70.4°, whereas unit *C* is almost perpendicular (77.1°) to the *B*−*B* dimer and presents a dihedral angle of 32.5° with the *A*−*A* dimer. This type of arrangement, which is unprecedented, resembles that observed in the *κ*-phases.[27,28] However, as schematically shown in Figure 4, the organic layers

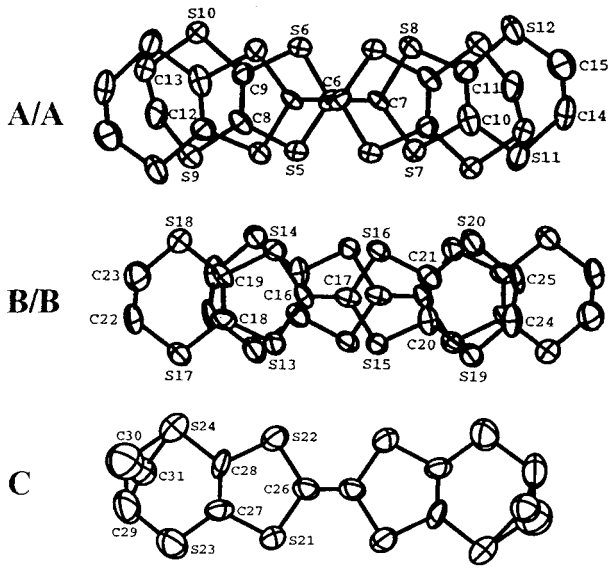

Figure 3. Atomic numbering and overlaps of the ET units within each $(ET)_2$ dimer in **1** (40% probability ellipsoids).

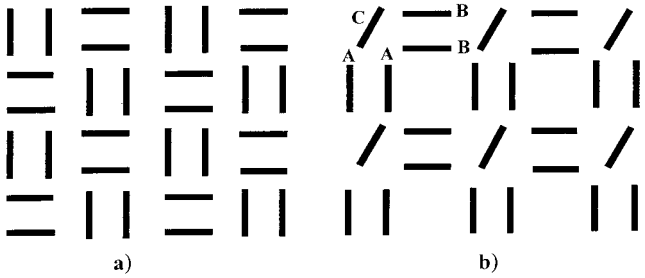

Figure 4. Schematic representation of the relationship between the organic packing in *κ*-phases (**a**) and in **1** (**b**) (projection views along the direction of the central C═C bond of the donor).

in **1** present an original packing which differs markedly from that of the *κ*-phases by the presence of the supplementary ET units, *C*. The latter induce a slippage of the adjacent *A*−*A* and *B*−*B* dimers of ca. 5 Å. The short S···S contacts observed between the organic molecules in **1** are close to those observed in *κ*-$(BEDT-TTF)_2X$ phases.[27,28] As indicated in Figure 2, only two short interdimer S···S distances are observed (3.37 and 3.55 Å), while unit *C*, which is surrounded by four dimer pairs, exhibits short S···S distances ranging 3.35−3.60 Å with both units *A* and *B*. The inorganic anions are located near the holes created by the slippage of the adjacent ET dimers (*A*−*A* and *B*−*B*) (Figure 2) in such a way that they are fairly well isolated from each other in the crystal. The minimum Cr···Cr interanion distance is 10.70 Å. On the other hand, the shortest sulfur−sulfur interanion separation is 4.24 Å, clearly greater than the sum of the van der Waals radii (3.6 Å). In contrast, there are three short contacts between the organic and inorganic layers [S(NCS)···S(ET), from 3.32 to 3.60 Å] (Figure 5).

Electronic Band Structure and Conductivity. Tight-binding band structure calculations of the extended Hückel type (experimental part) were carried out on a donor $(ET)_5$ two-dimensional layer, assuming the formal charge partitioning $[(ET)_5]^{4+}[Cr_2(C_2O_4)(NCS)_8]^{4-}$. With this formal oxidation for the organic *π* donor, there are six valence electrons per $(ET)_5$ unit to fill the five HOMO bands which are derived from the

(26) Masters, V. M.; Sharrad, C. A.; Bernhard, P. V.; Gahan, L. R.; Moubaraki, B.; Murray, K. S. *J. Chem. Soc., Dalton Trans.* **1998**, 413.

(27) Jung, D.; Evain, M.; Novoa, J. J.; Whangbo, M.-H.; Beno, M. A.; Kini, A. M.; Schultz, A. J.; Williams, J. M.; Nigrey, P. J. *Inorg. Chem.* **1989**, *28*, 4516.

(28) Doublet, M. L.; Canadell, E.; Shibaeva, R. P. *J. Phys. I* **1994**, *4*, 1479.

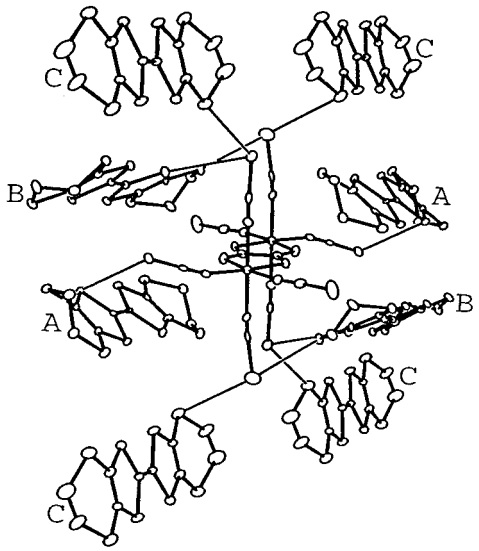

Figure 5. Perspective view of the anion environment (30% probability ellipsoids) showing the shortest S(ET)···S(NCS) contacts in **1**.

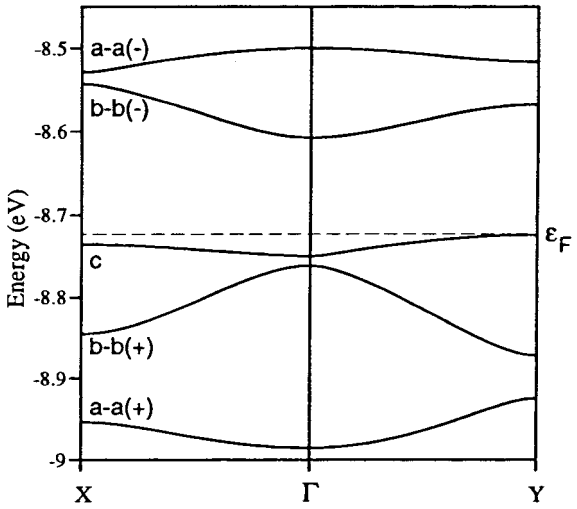

Figure 6. Dispersion energy of the HOMO bands for the $[(ET)_5]^{4+}$ layer in **1** along the wavevector directions $\Gamma \rightarrow X$ and $\Gamma \rightarrow Y$, where $\Gamma = (0,0)$, $X = (a^*/2, 0)$, and $Y = (0, b^*/2)$.

HOMOs of the five ET molecules. The intrastack and interstack interactions of the ET units lead to five bands, which are shown in Figure 6. With six electrons, the valence band structure is composed of three completely filled bands [$a-a(+)$, $b-b(+)$, c] and the conduction band structure is made of two empty bands [$a-a(-)$, $b-b(-)$]. To a first approximation, the intrastack interactions are responsible for the splitting between the in-phase and out-of-phase combinations of the HOMOs, whereas the interstack interactions are responsible for the dispersion of the bands along the wavevector directions of the reciprocal space. The lowest band $a-a(+)$ and highest band $a-a(-)$ derive almost exclusively from the bonding and antibonding combinations of the HOMOs of *A* units. In agreement with the structural data which shows that interatomic distances between ET units are shorter in $A-A$ than in $B-B$ dimers, a smaller splitting is observed for the bands $b-b(+)$ and $b-b(-)$, which mainly descend from the HOMOs of the *B* units (Figure 6). The upper filled band *c* derives largely from the HOMO of unit *C*. The band dispersion is rather weak, reflecting poor interstack interactions. Examination of the different interstack interactions indicates that the interaction of unit *C* is nearly negligible with the dimers $A-A$ and $B-B$. On the other hand, some weak

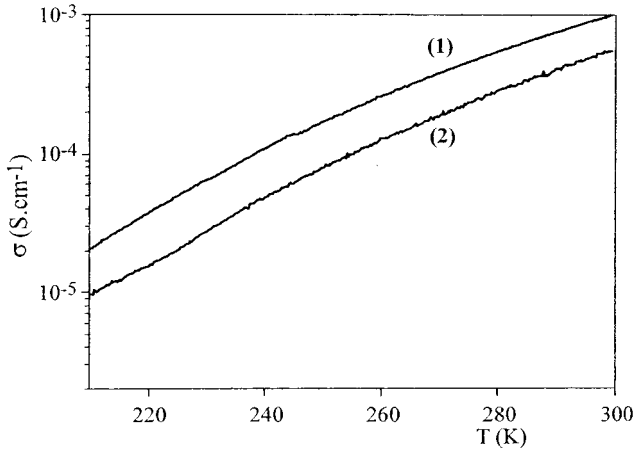

Figure 7. Temperature dependence of the d.c. electrical conductivity for **1** and **2**.

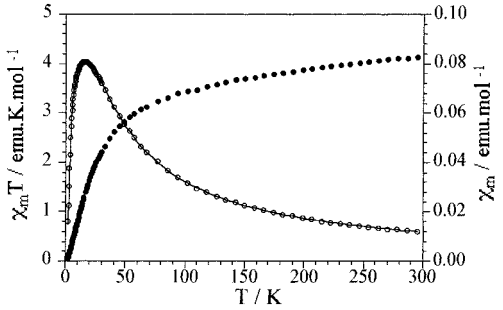

Figure 8. Thermal variation of the molar magnetic susceptibility, χ_m (○) and of the $\chi_m T$ (●) product of **1**. Solid line shows the best fit to the model (see text).

interactions occur between dimers $A-A$ and $B-B$. These weak interstack interactions are confirmed by the charges computed for the different components of the $[(ET)_5]^{4+}$ layer (+1.95, +1.95, and +0.10 for $A-A$, $B-B$, and *C*, respectively).[29,30] A band gap of 0.12 eV is computed for the $[(ET)_5]^{4+}$ slab. This is in agreement with the temperature dependence of conductivity performed on single crystals of compounds **1** and **2** since, in both cases, conductivity decreases when decreasing the temperature ($\sigma_{300K} \approx 10^{-3}$ S cm^{-1}) (Figure 7). This clearly indicates semiconducting properties; further analyses of the ln(resistivity) versus T^{-1} plot give straight lines from which linear fits give activation energies (E_a) of 0.23 and 0.25 eV for compounds **1** and **2**, respectively. These values are in agreement with the calculated gap.

Magnetic Properties. The magnetic susceptibility values measured in the range 2−300 K for both salts are given in the forms of χ_m versus *T* and $\chi_m T$ versus *T* plots for **1** (Figure 8) and in the form of $\chi_m T$ versus *T* plot for **2** (Figure 9), where χ_m is the molar magnetic susceptibility and *T* the temperature. For **1**, the χ_m versus *T* plot shows a maximum at ca. 16 K (Figure

(29) To verify the charge distribution of the ET units computed for $[(ET)_5]^{4+}$, we examined the C=C and the C−S bond lengths of the *A*, *B*, and *C* units, according to the procedure developed by Guionneau. P. et al.,[30] as suggested by the reviewers. The charges on the *A*, *B*, and *C* units are calculated to be +0.79, +0.92, and +0.64, respectively. These values are in good agreement with the total charge expected for the organic part (+4), but the individual charges appear to be not meaningful because of the limited quality of the crystal structure (bond length esd's greater than 0.01 Å[30]).

(30) Gionneau, P.; Kepert, C. J.; Bravic G.; Chasseau, D.; Truter, M. R.; Kurmoo, M.; Day, P. *Synth. Met.* **1997**, *86*, 1973. Ward, B. H.; Schlueter, J. A.; Geiser, U.; Wang, H. H.; Morales, E.; Parakka, J. P.; Thomas, S. Y.; Williams, J. M.; Nixon, P. G.; Winter, R. W.; Gard, G. L.; Koo, H.-J.; Whangbo, M.-H. *Chem. Mater.* **2000**, *12*, 343.

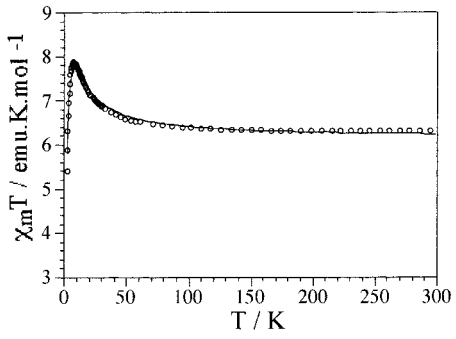

Figure 9. Thermal variation of the $\chi_m T$ product of **2**. Solid line represents the best fit to the model (see text).

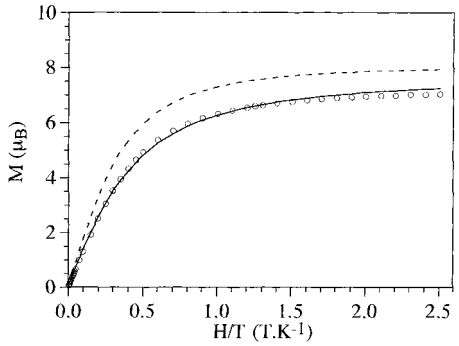

Figure 10. Magnetization versus magnetic field over temperature for **2** at 2 K. Dotted line represents the Brillouin function for an $S = 4$ spin state with $g = 2.00$. Solid line is the fit to the Brillouin function with a molecular field term (see text).

8), while $\chi_m T$ versus T plot reveals a continuous decrease from a value of 3.60 emu K mol^{-1} at 300 K, close to that calculated for two noninteracting Cr(III) (3.75 emu K mol^{-1}), to a value close to zero at 2 K. This is characteristic of the antiferromagnetic exchange interaction between the two chromium(III) centers. In contrast, for **2** the $\chi_m T$ product shows an increase from a value of 6.30 emu K mol^{-1} at 300 K to a value of 7.90 emu K mol^{-1} at 7 K and then sharply decreases down to 2 K (Figure 9). The room-temperature value is close to that expected for a pair of uncoupled Cr(III)−Fe(III) centers with an high-spin state of the iron(III) (6.25 emu K mol^{-1}), while the increase in $\chi_m T$ indicates that the Cr(III)−Fe(III) exchange interaction is ferromagnetic. These behaviors indicate that (i) the organic sublattice does not contribute to the magnetism since the four electrons on the ET radicals in both compounds are strongly antiferromagnetically coupled, and (ii) the magnetic coupling is antiferromagnetic between the two Cr(III) ions in compound **1** and ferromagnetic between the Cr(III) and the Fe(III) ions in compound **2**. To treat these data, we have used the susceptibility expressions derived for spin pairs (3/2−3/2 and 3/2−5/2 for **1** and **2**, respectively) coupled through an isotropic exchange interaction J (the Hamiltonian is written as $H = -2JS_1S_2$).[31] The best fits are plotted as solid lines in Figures 8 and 9. For **1**, the resulting fit (solid line in Figure 8) reproduces very satisfactorily, in the whole temperature range, the magnetic susceptibility with the following parameters: $g = 2.00$ and $J = -3.65$ cm^{-1}. The J value found in the fit is very close to those found for the Et_4N^+ salt of the same anion ($J = -3.23$ cm^{-1})[17] and in $(Et_4N)_4[Cr_2(C_2O_4)_5]0.2CHCl_3$ ($J = -3.1$ cm^{-1}), for which the X-ray study also shows a bis(bidentate) oxalato bridge.[26] For compound **2** containing the bimetallic anion ($S_1 = 3/2$ and $S_2 = 5/2$), the derived magnetic susceptibility equation, given in ref 31, includes contribution of a supplementary molecular field term, θ, that takes into account some antiferromagnetic interactions between dimers. To reduce the number of adjustable parameters we have used a mean g value in the fitting procedure. The resulting fit (solid line in Figure 9) reproduces quite well, in the whole temperature range, the $\chi_m T$ product of compound **2** with a set of parameters [$g = 1.985$, $J = 1.14$ cm^{-1}, and $\theta = -1.39$ K (-0.97 cm^{-1})] very close to that of the corresponding Et_4N^+ salt [$g = 1.973$, $J = 1.10$ cm^{-1}, and $\theta = -1.39$ K]. Rather than in the resulting θ value, emphasis is focused on the need of such parameters to explain the low temperature behavior for compound **2**; in fact, single-ion anisotropy effects should also contribute to this decrease in $\chi_m T$, and thus, θ only represents an effective parameter comprising these two effects.

To obtain further evidence of the $S = 4$ ground state of **2**, magnetization measurements were performed for **2**. A plot of the field dependent magnetization measurement at 2 K is presented in Figure 10, where M is plotted versus the applied magnetic field, H. The magnetization saturates at a value close to 7.0 μ_B, i.e., less than the expected value of 8.0 for an $S = 4$ spin state with a g value close to 2. Therefore, the Brillouin function for $S = 4$ and $g = 2.00$ (dotted line in Figure 10)[31] does not reproduce satisfactorily the experimental magnetization of compound **2**. The deviation is probably due to the presence of interdimer antiferromagnetic interactions, since the Brillouin function modified by the effective temperature $T^* = T - \theta$, taking into account such effects, leads to a better description of the experimental results with a $S = 4$ spin state, $g = 1.985$, and $\theta = -2.42$ K (solid line in Figure 10). This study therefore confirms the $S = 4$ ground state, and thus, the ferromagnetic intradimer coupling and the presence of the interdimer antiferromagnetic interactions.

The EPR spectrum of compound **1** (Figure 11a) shows, at room temperature, a quasi isotropic line centered at $g \approx 2.00$ (line width ≈ 320 G) that can be attributed to the Cr(III) dimer.[17] The intensity of this line increases as the temperature is decreased down to approximately 15 K, where the intensity of this signal starts an abrupt and continuous decrease down to the lowest temperature reached in the experiment (4.2 K). This behavior parallels that observed in the χ_m versus T plot and confirms that (i) the magnetic coupling between the Cr(III) ions is antiferromagnetic and (ii) the ET molecules do not contribute to the total magnetic moment, since no signal coming from the organic radicals can be observed. This absence of any signal from the ET units suggests that the electrons in the ET radicals must be strongly antiferromagnetically coupled in each dimer, which is in agreement with the electronic band structure calculations and the conductivity measurements given above. The EPR spectrum of **2** (Figure 11b) shows an intense and broad signal in the range 1000−2000 G and a second signal centered at 3500 G, both increase upon cooling. At the same time, other signals appear at high field upon cooling below 15 K. These signals together with the first dominant one correspond to the transitions between the lowest spin multiplet. This behavior is similar to that reported for the corresponding tetraethylammonium salt $[(C_2H_5)_4N]_4[CrFe(C_2O_4)(NCS)_8]$.[17] However, the signals in high field are more revealed for the ET salt; this is probably due to a better dilution of the magnetic inorganic dimer.

Conclusion

The two radical salts described here are the first ones obtained by the combination of the organic π donor ET with dinuclear magnetic anions.[18] Both are isostructural with a 1:5 stoichiometry and exhibit an unprecedented two-dimensional packing for

(31) Kahn, O. *Molecular Magnetism*; VCH Publishers: New York, 1993.

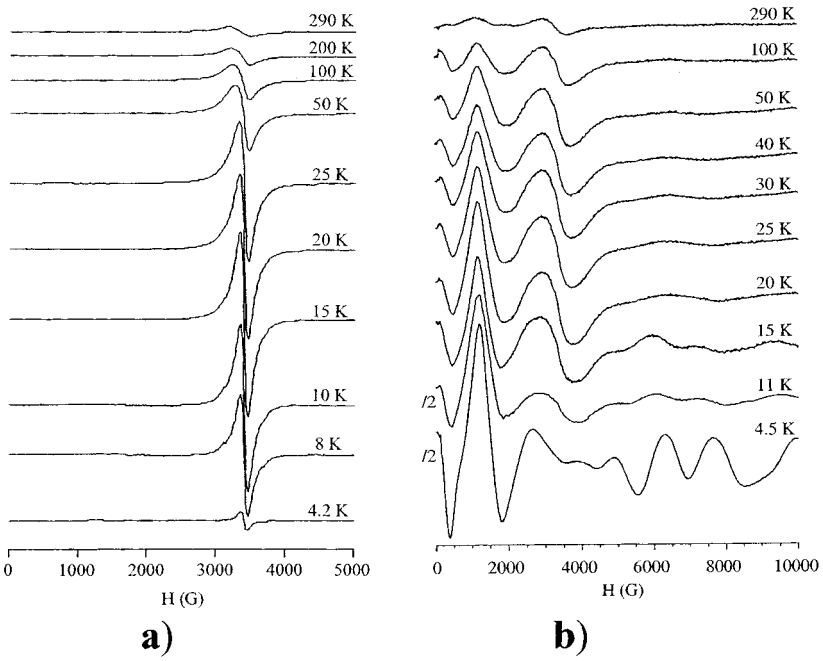

Figure 11. Temperature dependence of the EPR spectra for compounds **1** (a) and **2** (b).

the organic sublattice. In agreement with electronic band calculations and thermal variation of the conductivity, the magnetic measurements indicate that in both cases the two organic ET radicals of each dimer are strongly antiferromagnetically coupled and do not contribute to the magnetism. This is due probably to the short S···S contacts found in the crystal structure that allow the electron pairing of the radical units in each organic dimer. The magnetic exchange constants found in the anions are similar to those found in the corresponding tetraethylammonium salts, indicating that the organic part does not influence the M−M′ magnetic coupling. These observations suggest the lack of interaction between the two components. With the aim to favor the magnetic interactions between the organic and the inorganic parts, we are currently using these magnetic anions with new functionalized π-electron donors as hydroxy- and amino-tetrathiafulvalenes.[32,33] Such donors can participate in intermolecular hydrogen bonding and favor intermolecular interactions between the organic and the inorganic parts in the solid state.

Acknowledgment. This work was supported by the CNRS (Centre National de la Recherche Scientifique, UMR 6521), a French-Spanish Integrated Action (HF1997-0230 and 98059), the University of Brest (SUCRI 2E), and the Spanish "Ministerio de Ciencia y Tecnología" (Grant MAT98-0880). F.B. thanks the "Ministère de l'Education Nationale, de la Recherche et de la Technologie" for a postgraduate grant.

Supporting Information Available: One X-ray crystallographic file in CIF format. This material is available free of charge via the Internet at http://pubs.acs.org.″

IC010197B

(32) Binet, L.; Fabre, J.-M.; Becher, J. *Synthesis* **1997**, 26.
(33) Binet, L.; Fabre, J.-M. *Synthesis* **1997**, 1179.